

Elasticity Study in Ferromagnetic Shape Memory Alloys

Liyang Dai, James Cullen, Jun Cui and Manfred Wuttig
Department of Materials Science and Engineering,
University of Maryland,
College Park, Maryland, USA

ABSTRACT

The temperature dependences of the elastic constants of $\text{Ni}_{0.50}\text{Mn}_{0.284}\text{Ga}_{0.216}$ and Fe_3Pd were studied. Measurements were conducted by the ultrasonic continuous wave method. Anomalous behavior of the elastic constants temperature dependence in austenitic NiMnGa was observed, especially an abrupt 15% softening of C_{11} at the Curie temperature. The latter anomaly was found to be strongly influenced by the presence and orientation of applied magnetic fields. In martensitic NiMnGa, the temperature dependences of the velocities of all eleven elastic wave modes had abrupt changes at 220K, which indicate a structural phase change from the tetragonal to a second phase at lower temperature. The temperature and magnetic field effects in Fe_3Pd were also studied by the elastic constants measurements.

INTRODUCTION

Ferromagnetic shape memory alloys (FSMA) are a new class of active materials, which combine the properties of ferromagnetism with those of a diffusionless, reversible martensitic transformation. These materials have been scientifically interesting due to the possibility of inducing the shape memory effect with an external applied magnetic field. In these FSMA either inducing the austenite/ martensite transformation or rearranging the martensitic variant structure with an applied field will induce a reversible shape change. This effect has been named "ferromagnetic shape memory effect". While the former effect has been studied since the 1960's in martensitic steel and is relatively well understood, the latter has only recently received attention. The variant rearrangement phenomenon is a complicated one that depends on twin boundary mobility, the magnetic properties of the materials, proper biasing of the initial microstructure, proper specimen orientation, and specimen shape, among others. To date, Ni_2MnGa and Fe_3Pd are the only two alloys reported exhibiting giant (>0.5%) field-induced strain¹⁻⁴.

A great deal of work has accumulated that has detailed the characteristics of the martensitic transformation in these alloys^{2,5-7}. The dependence of a solid's elastic properties on temperature in the vicinity of a structural transformation provides insight into the nature of the transition and has been the focus of many studies⁸⁻¹³. It is often found that one of the shear moduli, most often $(C_{11}-C_{12})/2$, tends to decrease as the martensitic start temperature, M_s , is approached from above, in some cases becoming as small as one or two G Pa at the transformation temperature. This softening of the modulus is the result of the tendency of the crystal lattice to transform to a new structure that is obtainable from the austenite by a continuous deformation of the lattice.

Ni-Mn-Ga alloys with specific compositions develop a modulated structure^{10,11,14-17} at temperatures above the martensitic transition. This premartensitic transition is found to occur only for alloys with an electron to atom ration, e/a , less than 7.60. The relationship between the

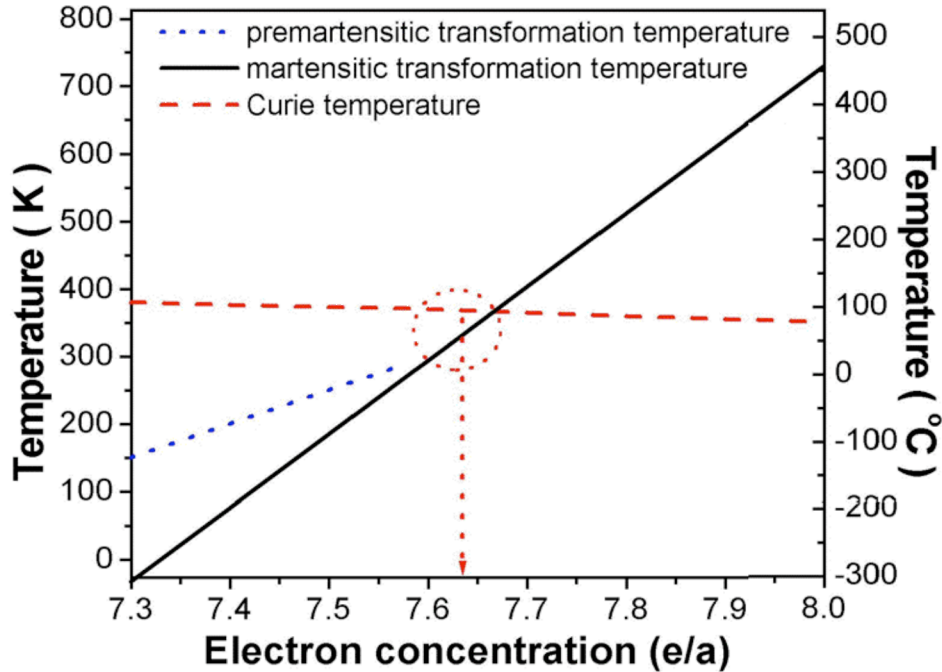


Figure 1 Schematic representation of the martensitic transformation, premartensitic transformation, and Curie temperature of NiMnGa alloys vs. concentration of valence electrons (e/a)¹⁰. The crystal investigated in this paper has a concentration of $e/a = 7.636$, as marked. It therefore falls into an intermediate region, where the premartensitic transformation temperature has merged with the martensite, which is still lower than the Curie temperature.

transformation temperatures and e/a ratio was schematically shown in Figure 1. The crystal we studied has a slightly higher e/a of about 7.64, which located at the joint area of the premartensitic and martensitic transformations. We therefore did not anticipate finding a premartensitic transition in it. In addition to the temperature near M_s , anomalous behavior of elastic moduli is expected to occur near the Curie temperature, T_C . Both ultrasonic investigations and neutron scattering studies of polycrystalline Ni-Mn-Ga alloys¹⁰ indicate that the slope of $E(T)$, the Young's modulus as function of temperature, changes near the Curie point.

In this paper we report the results of measurements of the elastic constants of a single crystal of $Ni_{0.50}Mn_{0.284}Ga_{0.216}$ from 488K down to 200K. Anomalies in the temperature dependences of all the constants were observed at T_C , as well as in the vicinity of M_s . In what follows, we describe our findings and discuss possible interpretations of the anomalous behavior of the bulk modulus at and below T_C . Recently study of the temperature dependence of the elastic constants in Fe_3Pd was discussed.

EXPERIMENT

Experiments were conducted with a Ni_2MnGa and Fe_3Pd single crystals.

The $Ni_{0.50}Mn_{0.284}Ga_{0.216}$ single crystal, which was grown by Adaptive Materials Technology, is a cuboidal sample, 10mm long on each side, had been oriented so that four opposing faces have a $\langle 110 \rangle$ normal, whereas the other two faces have a $\langle 100 \rangle$ normal. The crystal structure in the low temperature phase is tetragonal ($c/a=0.94$).

Small pieces were cut from this sample to perform supplementary SQUID and DSC measurements. According to the SQUID result, the Curie temperature is around 380K whereas the DSC measurements indicate a martensite start transformation temperature of 318K. The ultrasonic continuous wave method^{4,18-20} was used to determine the velocities of elastic waves in both austenitic and martensitic states of these alloys. All the elastic wave modes both in cubic and tetragonal crystals were listed in Table 1 and Table 2. In the tables, the \hat{W} , \hat{P} , \hat{H} mean the wave propagation, wave polarization and magnetic field directions, respectively.

Commercially available PZT based 1.5MHz pressure and shear transducers generated and detected the desired standing waves. A thin layer of vacuum grease was applied between the

Table 1 Elastic wave modes in cubic crystal²¹.

Modes	\hat{W}	\hat{P}	Elastic Constants: $C=\rho V^2$
L	[100]	[100]	C_{11}
T		[001], [010]	C_{44}
L	[110]	[110]	$(C_{11}+C_{12}+2C_{44})/2$
T_1		[001]	C_{44}
T_2		$[1\bar{1}0]$	$(C_{11}-C_{12})/2$
L	[111]	[111]	$(C_{11}+2C_{12}+4C_{44})/3$
T		$[11\bar{1}]$, $[1\bar{1}0]$	$(C_{11}-C_{12}+C_{44})/3$

Table 2 Elastic wave modes in tetragonal crystal²²

Modes	\hat{H}	\hat{P}	\hat{W}	Elastic Constants: $C=\rho V^2$
α	[001]	[001]	[001]	c_{33}
		[100]		c_{44}
β	[001]	[111]	[111]	$(2A-B+2C)^{-1}[C(c_{11}+2c_{66}+c_{12})+(2A-B)(2c_{44}+c_{13})]$
		$[1\bar{1}0]$		$(2A-B+2C)^{-1}[C(c_{11}-c_{12})+(2A-B)c_{44}]$
		[101]		$(2A-B+2C)^{-1}[2Cc_{44}+(2A-B)(c_{33}-c_{44}-c_{13})]$
π	[100]	[110]	[110]	$(A+C)^{-1}[Cc_{11}+A(2c_{44}+c_{13})]$
		[001]		$(A+C)^{-1}[Cc_{66}+Ac_{44}]$
		$[1\bar{1}0]$		$C^*=(A+C)^{-1}[Cc_{44}+A(c_{33}-c_{44}-c_{13})]$
γ	[001]	[110]	[110]	$(c_{11}+2c_{66}+c_{12})/2$
		$[1\bar{1}0]$		$C'=(c_{11}-c_{12})/2$
		[001]		c_{44}
κ	[100]	[001]	[001]	c_{11}
		[010]		c_{66}
		[100]		c_{44}

sample and the transducers. All measurements were conducted in a magnetic field of 0.8T applied in different crystalline direction, sufficiently large to create different single variants, so that the elastic modes as shown in Table 1 and Table 2 could be achieved. The measurements were taken as the temperature was lowered in the presence of the field.

According to the modes listed in Table 1 and Table 2, the elastic constants were over determined both in cubic and tetragonal phases.

RESULTS AND DISCUSSION

In the high temperature phase, austenitic phase, all four elastic constants of the cubic phase of the alloy have been determined from 428K down to and just below the onset of the Martensitic phase transition. In anticipation of the formation of two different orientations of a field-induced tetragonal crystal two field orientations were used, [100] and [001]. Figure 2 shows the temperature dependence of the elastic constants in austenitic $\text{Ni}_{0.50}\text{Mn}_{0.284}\text{Ga}_{0.216}$. The three symmetry constants, $C_{11}+2C_{12}$, $C_{11}-C_{12}$ and C_{44} show anomalous behavior near the Curie temperature, to varying extent. The shear constants undergo changes in slope right at T_C , while the C_{11} shows two very different behaviors in the two magnetic field orientations as shown in Figure 3. The softening of $C'=(C_{11}-C_{12})/2$ as the martensitic temperature is approached has been observed in prior studies in other NiMnGa alloys. Similar shear softening phenomena has also been found in other ferromagnetic alloys, such as CoNiGa and NiFeGa^{12,13}. The anomalies in C' and C_{44} are small in comparison with the variation in C_{11} at T_C , as can be seen in Figure 2. This combination of behaviors is somewhat similar to that often observed in Invar alloys like Fe-Ni²³ and Fe-Pt²³. They differ in that in the latter, C' shows the normal increase with decreasing temperature above the Curie point, leading to a maximum at T_C , while in the present study, C' decreases monotonically as the temperature is lowered, showing only a slight inflection at T_C .

The largest effect of the onset of magnetic order occurs in the temperature dependence of C_{11} , which contains both tetragonal shear and volume responses. However, it is the volume contribution that is most strongly effected at T_C . This becomes evident when the bulk modulus is calculated from the measured C_{11} and C_{12} . When the field was parallel to the propagation axis, there was a smooth variation in the bulk modulus through T_C . With the field perpendicular to the propagation direction, this modulus drops abruptly at T_C , and continues to decrease until the fall is interrupted at the Martensite temperature, M_S . The latter is similar to the anomalous behavior of the bulk modulus found in some invar alloys, such as FeNi^{24,25}, FePt²⁵, FeMn, and MnNiCr²⁴. In those alloys, the phenomena were explained as being due to volume magnetostriction. That mechanism, however, cannot explain the dependence on magnetic field orientation observed in our experiments. Instead, the orientation dependence leads us to propose that the Curie point also marks a transition between a cubic and a premartensitic phase, i.e., a modulated phase^{10,11,26}. The large difference between the $T < T_C$ behavior of the C_{11} mode with the field along two different $\langle 100 \rangle$ directions can be accounted for by assuming that the field reorients the modulation direction, in effect creating a tetragonal state. Thus the cubic C_{11} mode splits at the transition into two modes, similar to the splitting observed in that mode at the martensitic transition. We intend to make further measurements of the shear moduli with different field orientations to check this hypothesis.

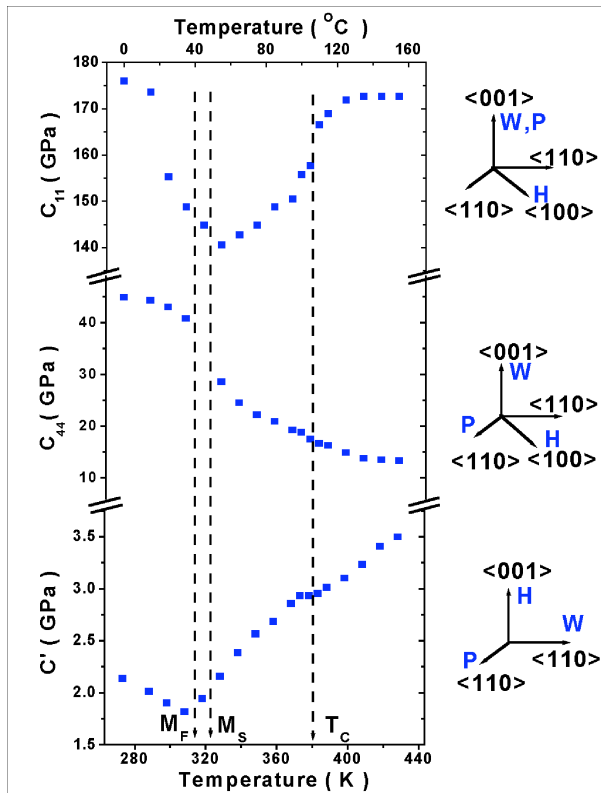


Figure 2 The elastic constants, C_{11} , C_{44} and C' , of $\text{Ni}_{0.50}\text{Mn}_{0.284}\text{Ga}_{0.216}$ vs. temperature. The propagation and polarization directions used to obtain the data are shown on the right.

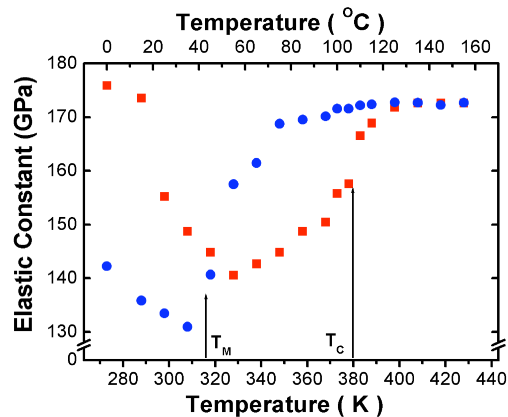


Figure 3 The elastic constant, converted from the wave velocity of the longitudinal wave along $\langle 100 \rangle$, is sensitive to the direction of applied magnetic field: The change of C_{11} is plotted vs. temperature. Measurements were taken with applied a 0.8 Tesla magnetic field along $\langle 001 \rangle$ (●) and $\langle 100 \rangle$ (■).

In the low temperature phase, martensitic phase, eleven velocities were measured and from them the six independent elastic constants were determined consistently. For example, C_{44} can be determined from three separate arrangements of magnetic field, wave propagation and polarization directions. They gave the same result within 2%. Figure 4 shows the temperature dependence of six of the modes so determined in the temperature range below the first martensitic transition, which is around 318K. C_{66} is very near C_{44} in that temperature range and

C_{33} shows similar behavior to C_{11} . All six elastic constants show the abrupt change around 220 K, clearly indicating that there is a transition from the tetragonal phase to another phase. The data below 220K in Figure 4 indicates the continuous change of the elastic wave velocities. They may not mean the same elastic constants with the first martensitic structure. We have no direct evidence for the nature of the new phase. However from our data we can give some insight into what it might be.

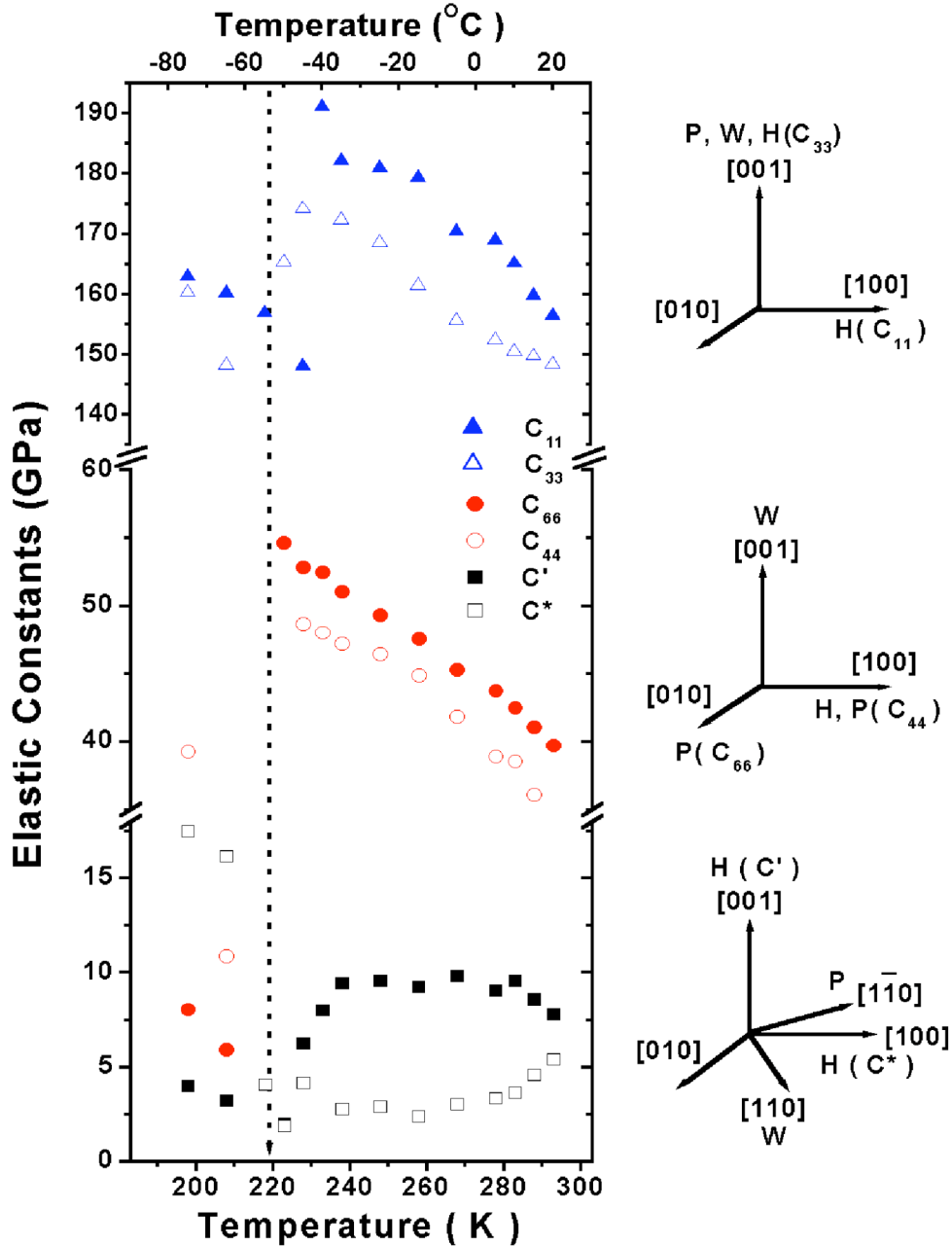


Figure 4 Temperature dependence of six elastic constants, C_{11} , C_{33} , C_{44} , C_{66} , C^* and C' , of $\text{Ni}_{0.50}\text{Mn}_{0.284}\text{Ga}_{0.216}$ below the first martensitic transformation temperature. C^* is defined in the Table. The propagation and polarization directions used to obtain the data are shown on the right. The field directions used to create the single-variant states are also shown. The data below 220K in Figure 4 indicates the continuous change of the elastic wave velocities.²⁷

Before we go into the details of the explanation, we display in Figure 5, a temperature, valence electron concentration (e/a) phase diagram, which we developed on the basis of these results and those of earlier work^{28,29}. The most important part of this diagram is in the regime of e/a around 7.636, because it shows that the plausible low temperature phase at this e/a ratio is the tetragonal phase with c/a greater than 1, while c/a is known to be less than one in the first tetragonal phase. We would now like to show that our data makes this a reasonable picture. To do this we refer to Figure 3, where we show the two smallest elastic constants over the entire temperature range starting from 380K. In the cubic phase they are degenerate and equal to C' , and below 318K they are split into two by the tetragonal distortion. The upper mode is the tetragonal C' mode, describing the stiffness of the tetragonal distortion in the xy plane. The lower, C^* , is actually a combination of the five elastic constants. Physically it represents the stiffness for further tetragonal distortion in the xz or yz planes. As the 220 K transition is approached, C' again goes soft and becomes degenerate with C^* . If only C' were getting soft in the tetragonal phase, one would expect the low temperature phase to be orthorhombic. However the fact that the C^* is also very small, indicates a reentrant behavior, that is, a return to the cubic phase ($c/a \rightarrow 1$) and then further distortion to a $c/a > 1$ phase at around 220K.

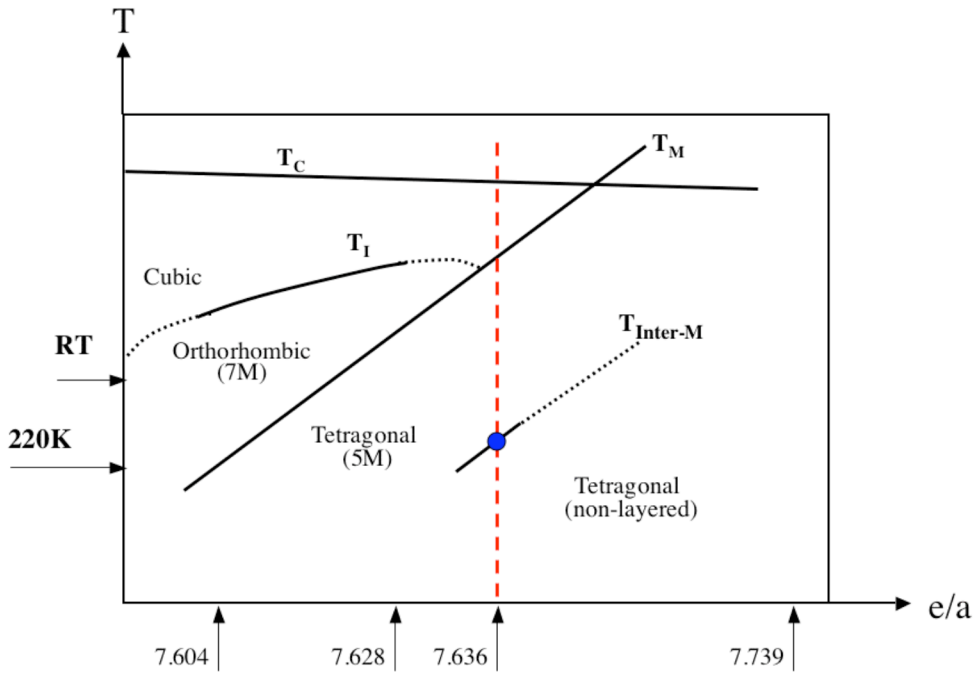


Figure 5 Schematic representation of structural and magnetic transformations in NiMnGa alloys vs. concentration of valence electrons (e/a). The different transformation temperatures, namely Curie point, Martensitic Transformation, Cubic to Orthorhombic transformation and inter-Martensitic transformation are depicted by T_C , T_M , T_I and $T_{Inter-M}$, respectively. The crystal investigated in this paper has a concentration of $e/a = 7.636$, as marked. The diagram was assembled with the help of the results obtained on three other crystals of similar composition^{28,29}. Their e/a ratios were marked on the diagram. According to our elastic constants data, we found the inter-martensitic transformation at around 220K. The tetragonal non-layered phase has $c/a > 1$. The dotted line was drawn so to allow the sample with $e/a = 7.74$ to be in the non-layered tetragonal phase at room temperature consistent with earlier work²⁷⁻²⁹.

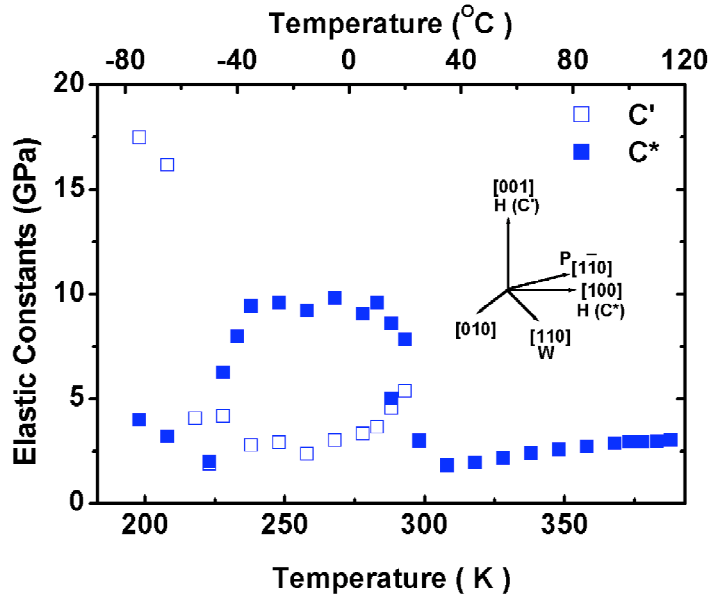


Figure 6 The elastic constants, C' and C^* were plotted vs. temperature from 380K (above the Curie point) to 200K. Measurements were taken with transverse waves along $[110]$ with polarization $[1\bar{1}0]$. C' was determined with magnetic field along $[001]$ (■); and C^* was determined with H parallel to $[100]$ (□). In the austenite, which is at the temperature higher than 318K, the two modes are degenerate. Notice how the C' mode drops rapidly below 233K, so that the two modes again degenerate at around 220K.²⁷

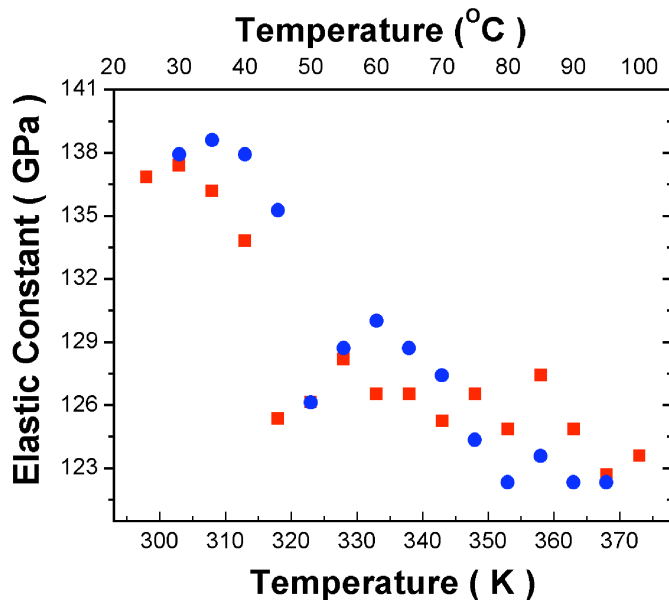


Figure 7 The temperature dependence of the elastic constant, C_{11} , in Fe_3Pd . The square and circle symbols marked the heating and cooling processes, respectively. Martensitic phase transition was found around 50°C by the elastic constants measurement.

In the study of Fe₃Pd single crystal, martensitic transformation was found by the temperature dependence of the elastic constants. Figure 7 shows the temperature dependence of C₁₁ in a Fe₃Pd single crystal. According to the DSC study³⁰, the abrupt change of C₁₁ in Figure 7 corresponds to the martensitic transition from the cubic phase to the tetragonal phase. This measurement was done with no magnetic field present.

The magnetic field induce phase change also was found in the Fe₃Pd single crystal. Magnetic field induced structure change has been found.

CONCLUSION

This paper reviewed the elastic constants study in the ferromagnetic shape memory alloys, Ni₂MnGa and Fe₃Pd. Measurements were conducted by the ultrasonic continuous wave method. The temperature dependence of the elastic constants of Ni_{0.50}Mn_{0.284}Ga_{0.216} and FePd was discussed. Anomalous behavior of the elastic constants temperature dependence in austenitic NiMnGa was observed, especially an abrupt 15% softening of C₁₁ at the Curie temperature. In martensitic NiMnGa, the temperature dependences of the velocities of all eleven elastic wave modes had abrupt changes at 220K, which indicate a structural phase change from the tetragonal to a second phase at lower temperature. The temperature and magnetic field effects in Fe₃Pd were also studied by the elastic constants measurements.

ACKNOWLEDGEMENT

This work was supported by the National Science Foundation, grant DMR0095166, and the Office of the Naval Research, contract No. MURI N000140110761.

REFERENCES

- 1 R. C. O'Handley, S. J. Murray, M. Marioni, H. Nembach, and S. M. Allen, *J. Appl. Phys.* 87, 4712-4717 (2000).
- 2 R. Tickle and R. D. James, *J. Magn. Magn. Mater.* 195, 627-638 (1999).
- 3 K. Ullakko, J. K. Huang, C. Kantner, R. C. O'Handley, and V. V. KoKorin, *Appl. Phys. Lett.* 69, 1966 (1996).
- 4 L. Dai, J. Cui, and M. Wuttig, *Smart Structures and Materials 2003: Active Materials: Behavior and Mechanics* (SPIE, Bellingham, WA, 2003) 5053, 595-602 (2003).
- 5 M. Wuttig, C. Craciunescu, and J. Li, *Mater. Trans. JIM.* 41, 933-937 (2000).
- 6 R. C. O'Handley, S. J. Murray, M. Marioni, H. Nembach, and S. M. Allen, *J. Appl. Phys.* 87, 4712 (1998).
- 7 P. J. Webster, K. R. A. Ziebeck, S. L. Town, and M. S. Peak, *Phil. Maga. B* 49, 295-310 (1983).
- 8 A. N. Vasilev, A. Kaiper, V. V. KoKorin, V. A. Chernenko, T. Takagi, and J. Tani, *JETP Lett.* 58, 306 (1993).
- 9 A. N. Vasilev, A. D. Bozhko, and V. V. Khovailo, *Phys. Rev. B* 59, 1113-1120 (1999).
- 10 V. A. Chernenko, J. Pons, C. Segui, and E. Cesari, *Acta Mater.* 50, 53-60 (2002).
- 11 V. A. Chernenko, V. A. L'vov, M. Pasquale, S. Besseghini, C. Sasso, and D. A. Polenur, *International Journal of Applied Electromagnetics and Mechanics* 12, 3-8 (2000).
- 12 T. E. Stenger and J. Trivisonno, *Phys. Rev. B* 57, 2735-2739 (1998).

13 J. Worgull, E. Petti, and J. Trivisonno, *Phys. Rev. B* 54, 15695-15699 (1996).
14 A. Planes, E. Obradó, and A. G.-C. a. L. Manosa, *Phys. Rev. Lett.* 79, 3926-3929 (1997).
15 L. Manosa and E. O. a. A. P. A. González-Comas, *Phys. Rev. B* 55, 11068-11071 (1997).
16 E. Obradó and L. M. o. a. A. P. A. González-Comas, *J. Appl. Phys.* 83, 7300-7302 (1998).
17 A. González-Comas, E. Obradó, L. Manosa, A. Planes, and A. Labarta, *J. Magn. Magn. Mater.* 196-197, 637-638 (1999).
18 D. I. Bolef and M. Menes, *J. Appl. Phys* 31, 1010 (1960).
19 M. Haluska, D. Havlik, G. Kirlinger, and W. Schranz, *J. Phys.: Condens. Matter* 11, 1009-1014 (1999).
20 M. Wuttig, L. Dai, and J. Cullen, *Appl. Phys. Lett.* 80, 1135-1137 (2001).
21 Kittel and Charles, *Introduction to solid state physics*, 4th ed. ed. (New York, Wiley, 1971).
22 K. Brugger, *J. Appl. Phys* 36, 759-773 (1964).
23 G. Hausch, *Journal of Physics F (Metal Physics)* 6, 1015-1023 (1976).
24 G. Hausch, *International Journal of Magnetism* 5, 111-114 (1973).
25 E. Torok and G. Hausch, *Physica Status Solidi A* 53, K147-K151 (1979).
26 U. Stuhr, P. Vorderwisch, V. V. Kokorin, and P.-A. Lindgard, *Phys. Rev. B* 56, 14360-14365 (1997).
27 L. Dai, J. Cullen, J. Cui, and M. Wuttig, Submitted to *J. Appl. Phys.* (2003).
28 A. Sozinov, A. A. Likhachev, N. Lanska, and K. Ullakko, *Appl. Phys. Lett.* 80, 1746-1748 (2002).
29 A. Sozinov, A. A. Likhachev, and K. Ullakko, *IEEE Trans. on Magnetics* 38, 2814-2816 (2002).
30 J. Cui, Thesis, University of Minnesota, 2002.